BIOCHEMISTRY
including biophysical chemistry & molecular biology

Article

pubs.acs.org/biochemistry

Protein Conformational Changes of the Oxidative Stress Sensor, SoxR, upon Redox Changes of the [2Fe−2S] Cluster Probed with Ultraviolet Resonance Raman Spectroscopy

Kazuo Kobayashi,*[,†] Misao Mizuno,[‡] Mayu Fujikawa,[†] and Yasuhisa Mizutani[‡]

[†]The Institute of Scientific and Industrial Research, Osaka University, Mihogaoka 8-1, Ibaraki, Osaka 567-0047, Japan

[‡]Graduate School of Science, Osaka University, 1-1 Machikaneyama, Toyonaka 560-0043, Japan

ABSTRACT: The [2Fe−2S] transcription factor, SoxR, a member of the MerR family, functions as a bacterial sensor of oxidative stress in *Escherichia coli*. SoxR is activated by reversible one-electron oxidation of the [2Fe−2S] cluster and enhances the production of various antioxidant proteins through the SoxRS regulon. Ultraviolet resonance Raman (UVRR) spectroscopic analysis of SoxR revealed conformational changes upon reduction of the [2Fe−2S] cluster in the absence and presence of promoter oligonucleotide. UVRR spectra reflected the environmental or structural changes of Trp following reduction. Notably, the environment around Trp91 contacting the [2Fe−2S] cluster was altered to become more hydrophilic, whereas that around Trp98 exhibited a small change to become more hydrophobic. In addition, changes in cation−π interactions between the [2Fe−2S] cluster and Trp91 were suggested. On the other hand, the environment around Tyr was barely affected by the [2Fe−2S] reduction. Binding of the promoter oligonucleotide triggered changes in Tyr located in the DNA-binding domain, but not Trp. Furthermore, conformational changes induced upon reduction of DNA-bound SoxR were not significantly different from those of DNA-free SoxR.

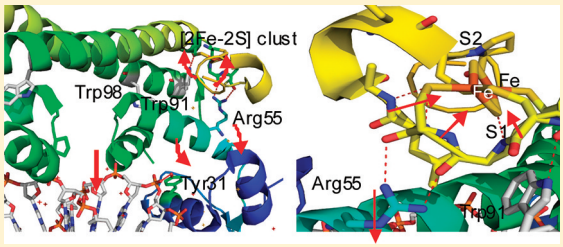

Signal transduction in sensor proteins is increasingly important in different research fields, and elucidation of the structural mechanism is a current focus of interest.[1,2] Sensor proteins are generally composed of a sensor domain and functional domain with a catalytic or DNA binding site for transcriptional activity. Binding of an external signal to the sensor domain induces slight alterations in structure, and subsequent conformational changes in the protein are propagated to the functional domain, leading to regulation of activity. Elucidation of these structural changes is thus essential to understand the mechanism of action of these proteins. One typical example is the mercury resistance operon regulator (MerR) family.[3−5] Members of the MerR family function as transcriptional activators in response to a variety of stress conditions, including exposure to heavy metals,[5−11] reactive oxygen species,[12,13] and antimicrobials.[14−19] Recent progress in genome sequencing has led to the identification of several MerR family members in bacterial genomes.[4] MerR proteins possess similar helix-turn-helix DNA binding motifs, a coiled-coil dimerization region, and a divergent C-terminal effector binding domain.[7,15,17] The structural diversity of the C-terminal domain allows individual MerR proteins to sense changes in the environment, such as metal ions, oxidative stress, and multidrug binding. In the absence of the appropriate signal, MerR-type transcription factors occupy suboptimally spaced promoter elements in the inactivated state. Upon activation, in response to the appropriate stimulus, these proteins undergo conformational changes that unwind the promoter region, allowing RNA polymerase to initiate transcription.[6,15,20,21]

SoxR, belonging to the MerR family, regulates the oxidative stress response to superoxide and nitric oxide in enteric *Escherichia coli* (*E. coli*) and *Salmonella enterica*. This unique transcription factor is a homodimer of 17 kDa subunits containing a [2Fe−2S] cluster essential for transcriptional activation of the *soxS* promoter.[12,13,22,23] Under conditions of oxidative stress, the metal center is oxidized and regulates *soxS* transcription via structural changes between the oxidized and reduced forms. Activated SoxR enhances the production of SoxS, a transcription activator, which controls the expression of >100 genes in the *SoxRS* regulon that collectively act to repair or avoid oxidative damage.[22,24,25]

The structure of *E. coli* SoxR complexed with a 20 bp oligonucleotide encompassing the majority of the *soxS* promoter region has been solved.[26] The structure reveals N-terminal winged helix DNA-binding, dimerization helix, and [2Fe−2S] cluster binding domains. The dimerization helix forms an antiparallel coiled coil that serves to stabilize the SoxR dimer. The [2Fe−2S] cluster of SoxR is coordinated to four cysteine residues (Cys119, Cys122, Cys124, and Cys130). One of the S atoms (S2) and two Fe atoms are fully exposed to solvent. The [2Fe−2S] cluster domain is further stabilized by interactions with helices of other subunits. The overall architecture of the SoxR−DNA complex is similar to those of other MerR proteins.[7,15,18] The DNA structure in the complex is in a bent conformation with local untwisting. SoxR in *E. coli*

Received: October 1, 2011
Published: October 11, 2011

contains two Trp and three Tyr residues. Trp91 is located near the [2Fe−2S] cluster of other subunit, whereas Trp98 in the α5 helix is stabilized via van der Waals contacts with conserved residues in the α3, α4, and α5 helices. Tyr31, Tyr49, and Tyr56 are located within the DNA-binding domain and thus used as probes to monitor protein conformational changes close to and distant from the [2Fe−2S] cluster. While the structure of transcriptionally activated SoxR has been solved, the molecular mechanisms through which redox changes of the [2Fe−2S] cluster induce protein conformational alteration and regulate transcription of the target promoter remain to be established. However, the lack of a SoxR structure in the reduced state limits our understanding of the structural transitions required for DNA binding and transcriptional activation.

To address this issue, we performed UV resonance Raman (UVRR) measurements of the oxidized and reduced forms of SoxR, in both the absence and presence of promoter oligonucleotide. UVRR spectroscopy is a powerful tool for monitoring protein structures and conformational changes.[27−30] Upon excitation at around 220−250 nm, side-chain vibrations of Tyr and Trp residues are selectively enhanced. UVRR bands of Trp and Tyr residues provide information on the hydrophobic/hydrophilic surroundings as well as hydrogen bonding.[27] In the current study, we first investigated conformational changes in SoxR upon reduction of the [2Fe−2S] cluster.

MATERIALS AND METHODS

Sample Preparation. Cloning of *E. coli* SoxR, construction of expression plasmids, and purification of wild-type (WT) protein were performed essentially as described previously.[31] Site-directed mutagenesis was performed using a PCR-based approach following the instructions of the Quik Change kit (Stratagene). SoxR protein samples were purified as the oxidized form, and confirmed as >95% homogeneous with SDS-PAGE. SoxR-DNA complexes were prepared according to the crystallization method described previously.[31] The palindromic oligonucleotide (GCCTCAAGTTAACTTGAGGC) purchased from Sigma Genosis Biotech Co., Ltd. (Japan) formed double-stranded DNA. Oligonucleotide was dissolved in aqueous solution containing 20 mM Tris-HCl (pH 7.6), 50 mM KCl, and 10 mM potassium/sodium tartrate, heated to 94 °C and gradually cooled to room temperature. For preparation of the SoxR-DNA complex, 40−50 μM SoxR (20 mM Mops, pH 7.6, 250 mM KCl, and 10 mM potassium/sodium tartrate) and oligonucleotide solutions were mixed at molar ratios of 2:1.05−1.1 and incubated for more than 4 h at 4 °C.[31]

For Raman measurements, the protein concentration was adjusted to 40−50 μM in 20 mM MOPS, pH 7.6, 0.25−0.5 M KCl, and 10 mM potassium/sodium tartrate. Reduced SoxR was prepared using the following method: a sample of SoxR was deoxygenated by repeated evacuation and flushing with nitrogen in a sealed cell. Sodium dithionite solution was added to the protein solution with a gastight Hamilton microsyringe under nitrogen atmosphere (final concentration, 0.5−1 mM). SoxR reduction was confirmed using visible absorption spectrophotometer.

UV Resonance Raman Measurements. UV probe pulses (20 ns, 1 kHz) at 230 nm were obtained by frequency quadrupling of the output of a Nd:YLF-pumped Ti:sapphire laser (Photonics Industries, TU-L). The probe power was kept as low as possible (0.5 μJ/pulse) to avoid photodamage of the protein sample. The probe beam was focused onto the sample cell with spherical and cylindrical lenses. Sodium sulfate (Na_2SO_4) (200 mM) was used as an internal intensity standard in all samples.

The sample solution was contained in a quartz 10 mm diameter NMR tube and spun with a spinning cell device designed to minimize off-center deviation during rotation. Raman scattering light was collected in the 135° backscattering geometry mode and focused onto the entrance slit of a custom-made Littrow prism prefilter (Bumko Keiki) coupled to a 55 cm single spectrograph (iHR550, Horiba Jobin-Yvon) equipped with holographic grating (2400 grooves mm^{-1}) using two achromatic doublet lenses. The prefilter effectively rejected stray background due to Rayleigh scattering and visible fluorescence. Dispersed light was detected with a liquid nitrogen-cooled CCD camera (SPEC-10:400B/LN, Roper Scientific) using the second diffraction order of the monochromator. Spectra were calibrated using the standard Raman spectra of cyclohexane.

Protein was replaced with a fresh sample every 5−10 min. The total exposure time to obtain a single spectrum was about 1 h. The integrity of the sample after exposure to UV laser light was carefully confirmed by comparing visible absorption spectra obtained before and after UVRR measurements.

RESULTS

Changes in the UVRR Spectra of SoxR Excited at 230 nm upon Reduction of the [2Fe−2S] Clusters. Raman bands arising from Trp and Tyr residues are selectively enhanced upon excitation around 220−250 nm and can be used as structural probes for their surroundings.[27] Figure 1 depicts raw UVRR spectra of the oxidized and reduced forms of WT SoxR. Trp and Tyr bands in UVRR spectra were identified by comparison with spectra of aqueous amino acid solutions.[27] The raw spectrum was dominated by bands arising from two Trp (Trp91, 98) and three Tyr (Tyr31, 49, 56) residues (labeled W and Y, respectively, followed by the mode number).[27] Since the protein concentrations were the same in all measurements performed at a given excitation wavelength, the intensities of the Raman features were comparable in all raw spectra.

Reduction of the [2Fe−2S] cluster of SoxR caused intensity changes and frequency shifts in Trp vibrational modes (Figures 1a,b). To further clarify the spectral changes, difference spectra were calculated so that the band for SO_4^{2-} (981 cm^{-1}), present at the same concentration as the internal intensity standard, was taken as zero. The difference spectrum yielded the following data: 757(+)/767(−) cm^{-1} (W18), 1004(−)/1012(+) cm^{-1} (W16), 1558(−)/1569(+) cm^{-1} (W3) (Figure 1d).

The WT spectrum arises from contributions of both Trp91 and Trp98. To identify the specific Trp residue responsible for spectral changes in WT, we performed UVRR measurements on SoxR proteins in which one of the two Trp residues was substituted with Phe. The W98F mutant (Trp91) contained low levels of [2Fe−2S] centers. The mutation of Trp98 may have compromised their structural integrity such that handling during purification. Therefore, we could not perform Raman measurement of Trp91. The spectrum for Trp91 was obtained by subtracting that of W91F mutant (Trp98) from that of WT under the assumption that the environment of Trp98 in W91F is not affected by the mutation.

The difference spectra of the reduced minus oxidized forms were compared for Trp91 and Trp98 (Figure 1e,f). Interestingly, spectral changes of Trp91 were distinct from

dx.doi.org/10.1021/bi201526y | Biochemistry 2011, 50, 9468−9474

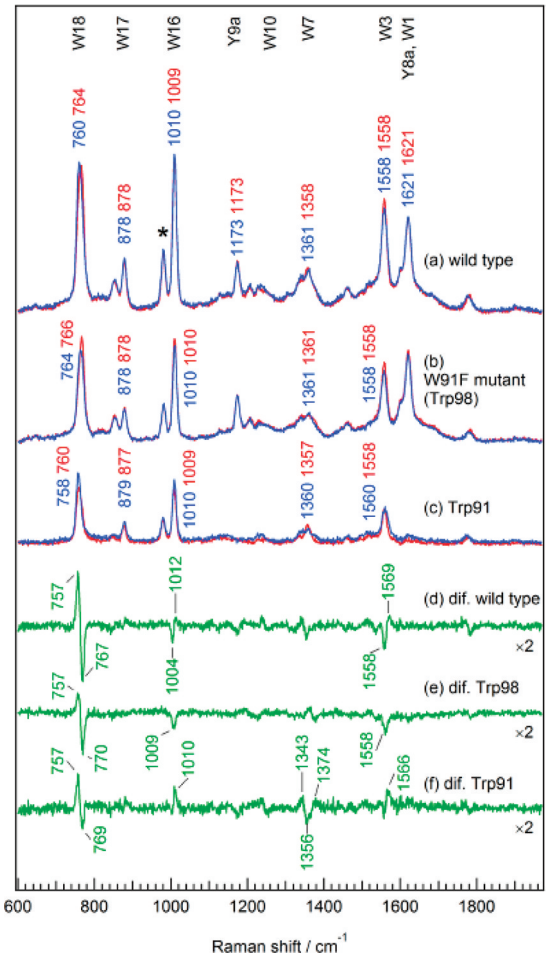

Figure 1. The 230 nm excited UVRR spectra of WT (a) and W91F mutant (Trp98) (b) of SoxR. Spectra of the oxidized (red line) and reduced forms (blue line) are shown. The spectrum of Trp91 (c) was calculated from that of WT minus that of W91F. The reduced minus oxidized spectra for WT (d), Trp98 (e), and Trp91 (f) are shown.

those of the Trp98, except for a frequency shift of the W18 band, which is commonly observed for the two Trp residues. The difference spectrum of Trp91 yielded positive peaks at 1010 (W16) and 1343 cm^{-1} (W7), indicating an increase in the intensity of Trp bands in the reduced form, compared with the oxidized form. In contrast, the difference spectrum of Trp98 yielded negative peaks at 1009 (W16) and 1558 cm^{-1} (W3). Peaks at around 1010 and 1560 cm^{-1} were thus derived from the intensity differences in the two Trp residues. In addition, the difference spectrum of Trp91 exhibited a positive band at 1374 cm^{-1}, suggesting the appearance of a high-frequency component of the W7 band. This type of frequency perturbation is likely to arise from steric repulsion between the indole ring and its environment.[32] A similar frequency shift observed for the Trp W7 band in bacteriorhodopsin has been attributed to repulsion between the indole ring and methyl groups of retinal chromophore.[33]

The positive/negative peaks at 1340/1360 cm^{-1}, arising due to the intensity of the low- and high-frequency components, were increased and decreased, respectively, for Trp91. The W7 band of Trp usually splits into a doublet at 1360/1340 cm^{-1} owing to Fermi resonance between a fundamental mode and a combination of two out-of-plane modes involving benzene and pyrrole rings comprising the Trp side chain.[32,34,35] The intensity ratio, $R(I_{1360}/I_{1340})$, is sensitive to the polarity of the environment around Trp residues.[35] The R value for solvent-exposed Trp is the lowest value measured at $\leq$1.1, while the R values for least polar environments similar to ethanol and dioxane are >1.5.[32] The R values for Trp91 and Trp98 in the oxidized state were 2.0 and 1.0, respectively. This finding suggests that Trp91 is buried in a more hydrophobic environment than Trp98. Upon SoxR reduction, the R value for Trp91 was remarkably decreased to 1.2, whereas that for Trp98 exhibited a relatively limited increase to 1.2. These results suggest that upon reduction the environment around Trp91 changes significantly to become more hydrophilic while that around Trp98 undergoes a small change to become more hydrophobic.

The W3 frequencies of Trp are sensitive to the absolute value of torsion angle ($\chi^{2,1}$) about the C_β–C_3 bond connecting the indole ring to the peptide main chain.[36−38] The W3 frequency of Trp98 at 1558 cm^{-1} corresponded to a $\chi^{2,1}$ angle of 120°.[36,39] This value is close to the X-ray-determined torsion angle of 111°.[26] On the other hand, the W3 frequency of 1560 cm^{-1} for Trp91 was higher than that predicted, based on crystallographic data. The difference spectrum exhibited a positive band at 1566 cm^{-1}. Conversely, the difference spectrum of Trp98 W3 showed a negative band at 1558 cm^{-1}.

In contrast to the data obtained with Trp, we observed no changes in Tyr Raman bands, including Y1, Y9a, Y7a, Y8b, and Y8a, upon reduction of WT, suggestive of no alterations in the Tyr (Tyr31, Tyr49, Tyr56) environment of WT protein upon reduction.

UVRR Spectra of SoxR Excited at 230 nm upon Binding of Promoter DNA. Figure 2 presents the UVRR spectra of oxidized, reduced, DNA-bound oxidized, and DNA-bound reduced forms of the protein (a) excited at 230 nm and the difference spectra (reduced minus oxidized) of the DNA-free forms (b), DNA-bound forms (c), DNA-bound minus DNA-free oxidized forms (d), and DNA-bound minus DNA-free reduced forms (e). DNA binding to the SoxR protein induced changes in several negative peaks. The negative bands at 1174, 1602, and 1617 cm^{-1} resulted from reduction in the intensities of Y9a, Y8b, and Y8a. This finding is indicative of alterations in the environment around Tyr residues upon DNA binding. To identify the specific Tyr residue(s) contributing to spectral changes in WT protein, each of the three Tyr residues was mutated to Phe. However, these mutants contained only low levels of [2Fe−2S] centers, and therefore, we could not perform Raman measurements. In contrast, Trp Raman bands exhibited small spectral changes (except intensity reduction of 1010 cm^{-1} (W16) and 1560 cm^{-1} (W3)), suggesting that Trp residues undergo minor environmental changes. The positive peak at 1485 cm^{-1} observed in the presence of DNA was attributed to the Raman band of oligonucleotide.[40−42]

Notably, the difference spectrum between the reduced and oxidized DNA-bound forms resembled that of the DNA-free form (Figure 2b,c). Thus, it appears that the conformational changes induced upon reduction of DNA-bound SoxR are not significantly different from those in the DNA-free form.

DISCUSSION

Conformational Changes in Trp and Tyr Residues upon Reduction of [2Fe−2S] Clusters of SoxR. The SoxR protein contains two Trp residues at positions 91 and 98. Both Trp residues are involved in long dimerization of the α5 helix and play structurally and functionally important roles.

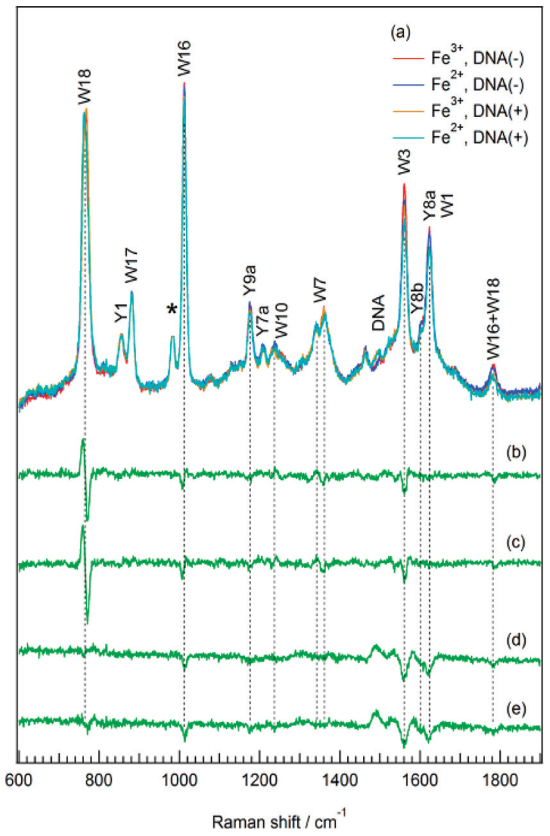

Figure 2. The 230 nm excited UVRR spectra of DNA-free forms of the oxidized and the reduced and DNA-bound forms of the oxidized and the reduced SoxR (a). The difference spectra: reduced minus oxidized in the DNA-free forms (b), reduced minus oxidized in the DNA-bound forms (c), DNA-bound minus DNA-free in the oxidized forms (d), and DNA-bound minus DNA-free in the reduced forms (e).

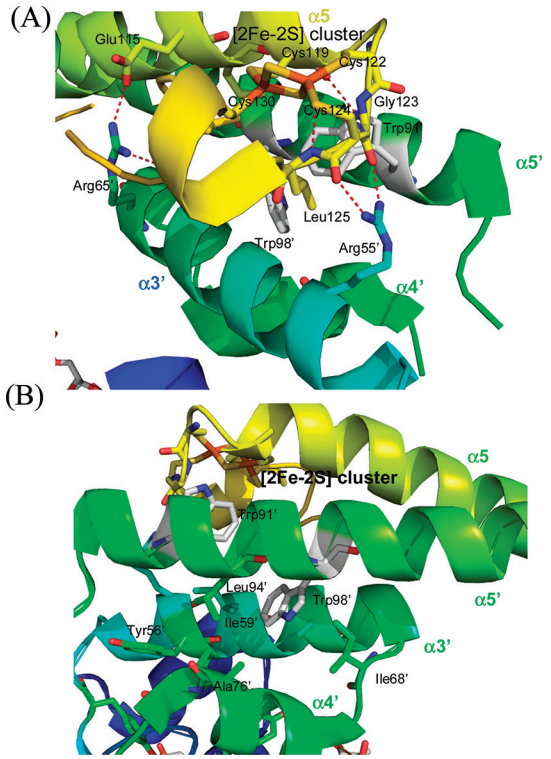

Figure 3. Crystallographic structure of SoxR. Close-up of the region near Trp 91 (A) and Trp98 (B) residues. These structures were produced with PyMol using a structure from the Protein Data Bank (PDB ID 2ZHG: ref 26).

Magnified images of the region near the Trp residues are presented in Figure 3A,B. Trp91, a conserved residue among SoxR proteins, is located in close proximity to the [2Fe−2S] cluster of other subunit, and the $N_{\varepsilon 1}$ atom of indole forms a hydrogen bond with the backbone carbonyl of Cys119 coordinated to the [2Fe−2S] cluster in the $\alpha 5'$ (where the prime indicates the other subunit) helix. On the other hand, Trp98 (also highly conserved but replaced with Leu in *S. pomeroyi* SoxR) is located so that the $\alpha 5$ helix is stabilized by hydrophobic interactions with conserved residues in the $\alpha 3$ and $\alpha 4$ helices. In the present study, the two Trp residues were employed to probe tertiary structure changes in the protein conformation upon reduction of the [2Fe−2S] cluster. Our UVRR data showed that both Trp91 and Trp98 undergo intensity changes and frequency shifts upon reduction, supporting significant environmental changes. The decreased I_{1360}/I_{1340} ratio for Trp91 clearly suggests that the surrounding environment becomes more hydrophilic in the reduced state, implying partial exposure of this residue to solvent. On the other hand, hydrophobicity in the Trp98 environment is increased to a small extent. Reduction of the [2Fe−2S] cluster may accompany the relative orientations of $\alpha 3$, $\alpha 5$ and $\alpha 4$ helices, and cause tightness of the nonbonded contacts of Trp98. Since no frequency shift was observed for the hydrogen bond marker band (W17 at 878 cm^{-1} [34] and W10 at 1237 cm^{-1} [43]), we propose that the hydrogen bond between Trp91 and the backbone carbonyl of Cys119 is barely affected.

W16 (benzene ring-breathing mode) and W18 (indole ring-breathing mode) are sensitive to an electronic state of the aromatic ring. Model studies have shown that increases in solvent dielectric constant and hydrogen-bonding strength lower the frequencies of these bands.[44−46] Since no frequency shift was observed for the hydrogen bond marker band (W17 and W10) in the present data, the frequency change of the W18 band can be ascribed to changes in the hydrophobicity of Trp. In addition, the intensity changes in the W16 band have been characterized for not only hydrophobicity but also cation−Trp π interactions in both proteins and small molecule model systems,[32,47−49] where the cations involve metal ions[47] and protonated imidazole of His.[48,49] In our experiments, frequency changes in the W18 bands were commonly observed for Trp91 and Trp98, whereas spectral changes in the W16 band in Trp91 were distinct from that of Trp98 (Figure 1e,f). These results suggest that electrostatic interactions between the [2Fe−2S] cluster and π orbital of the indole side chain, with the closest distance of about 4.5 Å, contribute to the W16 band intensity of Trp91. The observed increase in Trp91 W16 intensity can be interpreted as a decrease in cation−π interactions upon reduction.

The W3 frequency of Trp residue is correlated with the Trp $\chi^{2,1}$ dihedral angle.[36−38] The dihedral angle, predicted based on the W3 frequencies of Trp98, was similar to that determined using X-ray crystallography.[26] However, the W3 band frequency of Trp91 was high. The frequency of the W3 vibration of Trp91 was further upshifted upon reduction. Juszczak and Desamero proposed that weak electrostatic interactions, such as anion−quadrupole, cation−π, and

dx.doi.org/10.1021/bi201526y | *Biochemistry* 2011, 50, 9468−9474

aromatic face−edge interactions, influence the W3 frequency of Trp.[38] Similarly, electrostatic interactions between the [2Fe−2S] cluster and π orbital of indole side chain may contribute to the W3 band frequency of Trp91. The further upshift in the reduced state of the protein may be attributed to changes in interactions between the [2Fe−2S] cluster and Trp residue.

Our UVRR results showed that Tyr residues experience no alterations upon redox change, clearly suggesting that hydrogen bond and nonbonded contacts of Tyr residues with neighboring amino acids are not affected upon reduction.

Conformational Changes upon DNA Binding. Upon binding of SoxR to DNA, the DNA-binding domain undergoes an outward rotation of ~9°, and the Fe−S cluster-binding domain receives an outward rotation of ≈6°, resulting in widening of the distance between the α2 and α2′ helices. The α5 helix connecting both domains exhibits an inner helical twist, leading to a change in the relative positions of dimerization helices.[26] UVRR results disclose that Trp residues undergo small environmental changes upon DNA binding, consistent with the X-ray crystal structure showing that the hydrogen bond of Trp91 and nonbonded contacts of Trp91 and Trp98 are not affected. This finding suggests that the individual domains of DNA-free and -bound SoxR do not present significant structural differences. An analogous set of interactions has been reported for the MerR family of drug-bound BmrR−DNA complexes.[50] Upon DNA binding, BmrR undergoes conformational changes in terms of remodeling of the coiled-coil α5 helix and significant inward movement of the wing. However, the individual DNA-binding and drug-binding domains of DNA-free and DNA-bound BmrR are structurally similar.

Following DNA binding, UVRR spectra of the protein exhibited significant changes in terms of Tyr, but not Trp bands. Parts A and B of Figure 4 depict magnified images of the environment of Tyr residues in the DNA-free and bound forms, respectively. Tyr31 in the DNA recognition helix (α2) and Tyr49 in the loop between helices α2 and α3 are absolutely conserved among not only SoxR proteins but also other members of the MerR family, including MerR, CueR, ZntR, Mta, and BmrR. Tyr56 in the α3 helix is not conserved and exposed to solvent. In the DNA-free form, OH of Tyr31 forms a hydrogen bond with nitrogen of Gln64. Upon DNA binding, rotation of Tyr31 is accompanied by rearrangement of the hydrogen bond from Gln64 to the phosphate backbone of DNA. On the other hand, Tyr49 forms hydrogen bonds with Arg47 and Glu32 in the DNA-free protein. Upon DNA binding, Tyr49 is surrounded by hydrophobic residues, concomitant with cleavage of the hydrogen bond. Instead, Arg47 donates a hydrogen bond to the phosphate backbone DNA and may be functionally important in stabilizing the activated DNA conformation.[26] Similar conformational changes have been reported for other proteins of the MerR family, including BmrR,[50] MtaN,[17] and MerR.[51] UVRR results revealed decreased intensities of the Y9a, Y8b, and Y8a bands. Model compound studies have clarified that the intensity and frequency of Tyr bands are influenced by the strength of the hydrogen bond.[52,53] Therefore, it is reasonable to assume that the changes in hydrogen bonding of Tyr49 trigger spectral changes upon DNA binding.

Conformational Changes of Trp and Tyr Residues upon Reduction of DNA-Bound SoxR. UVRR spectral data indicate that the conformational changes upon reduction of DNA-bound SoxR are not significantly different from those of the DNA-free form. This result has important implications for the function of SoxR. Reduction of the [2Fe−2S] cluster triggers significant changes in the environment around Trp91 and Trp98, which may induce interdomain reorganization required for DNA distortion. However, this process does not affect the environment around Tyr31, Tyr49, and Tyr56. Notably, the hydrogen bond interaction between Tyr31 in the α2 helix and the phosphate backbone of DNA remains unaltered in the reduced form, suggesting that this bond is not important for redox-dependent regulation of structural transition in the activated DNA conformation.

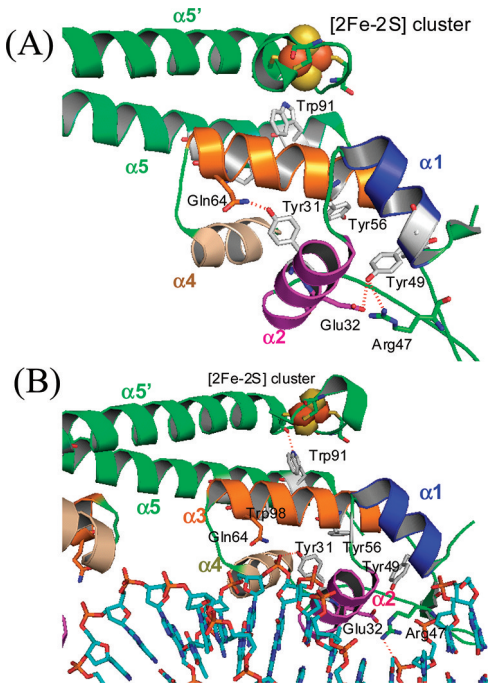

Figure 4. Crystallographic structure of SoxR. Close-up the region near the Tyr residues (A) DNA-free form of SoxR. (B) SoxR−*soxS* promoter complex. These structures were produced with PyMol using a structure from the Protein Data Bank (PDB ID 2ZHG and 2ZHH: ref 26).

Electrochemical studies have shown that the reduction potential of SoxR bound to the promoter DNA is positively shifted dramatically from −290[22] to 200 mV.[54] The shift (490 mV) is possibly derived from the conformational distortion induced by binding of reduced SoxR to DNA. The coordinate and electronic structures of the [2Fe−2S] cluster of SoxR are altered upon DNA binding but do not directly reflect changes in the Trp environment.

Propagation of Structural Changes from the [2Fe−2S] Cluster to DNA Distortion. Structural alterations of the [2Fe−2S] cluster of SoxR induced by redox changes are communicated to the DNA-binding domain, leading to target promoter DNA distortion. The redox-dependent structural fluctuation of [2Fe−2S] cluster proteins has been studied in oxidized and reduced ferredoxin and putidaredoxin structures with high-resolution X-ray crystallography.[55,56] In both proteins, the [2Fe−2S] cluster is shielded from the solvent by surrounding residues. The bridging and cysteinyl sulfur atoms are hydrogen-bonded to the backbone amide. Reduction of the prosthetic group significantly affects this hydrogen bond. The additional negative charge on the sulfur atoms attracts the amides of the main chain and increases charge repulsion with

the oxygen atom. This is consistent with theoretical calculations, where most of the added charge in the reduced [2Fe−2S] cluster is evenly distributed between the bridging and cysteinyl sulfur atoms and compensated by the NH--S hydrogen bond.[57] In the [2Fe−2S] cluster of SoxR, the lower sulfur atom (S1) is hydrogen-bonded to the amide of Gly123 and displays van der Waals interactions with amides of Cys124 and Leu125, whereas the other side of S2 is fully exposed to solvent. Upon reduction, an additional negative charge on the S1 atom may attract main-chain amides. The conformational changes affect the [2Fe−2S] cluster binding loop of Gly123, which, in turn, would pull up Arg55′ in the α3′ helix, thereby altering the structure of the DNA-binding domain. The above sequential events may induce considerable changes in the Raman spectra of Trp91. An analogous set of events in drug-bound BmR−DNA complex appears crucial for transcription activation. These interactions may thus be common to all MerR family regulators.[58]

■ CONCLUSIONS

UVRR analysis of the oxidized and reduced forms of the [2Fe−2S] transcription factor, SoxR, has facilitated new insights into the structural basis of the general mechanism of transcriptional activation by the MerR family. Our results support significant environmental changes for Trp91 and Trp98 in the long dimerization region upon reduction. In contrast, the environment around Tyr in the DNA-binding domain is barely altered. These findings confirm the importance of interactions between Trp91 and the [2Fe−2S] cluster binding loop.

■ AUTHOR INFORMATION

Corresponding Author

*E-mail: kobayasi@sanken.osaka-u.ac.jp. Tel: 81-6-6879-8501. Fax: 81-6-6879-4889.

Funding

This work was supported by Grant-in aid from the Ministry of Education, Culture, Sports, Science, and Technology of Japan.

■ ACKNOWLEDGMENTS

We thank Dr. Satoshi Watanabe in Kyoto University for stimulating discussions. We are additionally grateful to Dr. Yu Hisano from the Institute of Scientific and Industrial Research, Osaka University, for experimental support.

■ REFERENCES

(1) Rodgers, K. R. (1999) Heme-based sensors in biological systems. *Curr. Opin. Chem. Biol. 3*, 158−167.

(2) Gilles-Gonzalez, M.-A., and Gonzalez, G. (2005) Heme-based sensors: defining characteristics, recent developments, and regulatory hypotheses. *J. Inorg. Biochem. 99*, 1−22.

(3) O'Halloran, T. V. (1993) Transition metals in control of gene expression. *Science 261*, 715−725.

(4) Brown, N. L., Stoyanov, J. V., Kidd, S. P., and Hobman, J. L. (2003) The MerR family of transcriptional regulators. *FEBS Microbiol. Rev. 27*, 145−163.

(5) O'Halloran, T. V., Frantz, B., Shin, M. K., Ralston, D. M., and Wright, J. G. (1989) The MerR heavy-metal receptor mediates positive activation in a topological novel transcription complex. *Cell 56*, 119−129.

(6) Outten, C. E., Outten, F. W., and O'Halloran, T. V. (1999) DNA distortion mechanism for transcriptional activation by ZntR, a Zn(II)-responsive MerR homologue in *Escherichia coli*. *J. Biol. Chem. 274*, 37517−37524.

(7) Changela, A., Chen, K., Xue, Y., Holschen, J., Outten, C. E., O'Halloran, T. V., and Mondragón, A. (2003) Molecular Basis of Metal-Ion Selectivity and Zeptomolar Sensitivity by CueR. *Science 301*, 1383−1387.

(8) Frantz, B., and O'Halloran, T. V. (1990) DNA distortion accompanies transcriptional activation by the metal-responsive gene-regulatory protein MerR. *Biochemistry 29*, 4747−4751.

(9) Checa, S. K., Espariz, M., Audero, M. E., Botta, P. E., Spinelli, S. V., and Soncini, F. C. (2007) Bacterial sensing of and resistance to gold salts. *Mol. Microbiol. 63*, 1307−1318.

(10) Lee, S. W., Glickmann, E., and Cooksey, D. A. (2001) Chromosomal Locus for Cadmium Resistance in *Pseudomonas putida* Consisting of a Cadmium-Transporting ATPase and a MerR Family Response Regulator. *Appl. Environ. Microbiol. 67*, 1437−1444.

(11) Borremans, B., Hobman, J. L., Provoost, A., Brown, N. L., and van Der Lelie, D. J. (2001) Cloning and Functional Analysis of the *pbr* Lead Resistance Determinant of *Ralstonia metallidurans* CH34. *J. Bacteriol. 183*, 5651−5658.

(12) Hidalgo, E., and Demple, B. (1994) An iron-sulfur center essential for transcriptional activation by the redox-sensing SoxR protein. *EMBO J. 13*, 138−146.

(13) Wu, J., Dunham, W. R., and Weiss, B. (1995) Overproduction and physical characterization of SoxR, a [2Fe-2S] protein that governs an oxidative response regulon in *Escherichia coli*. *J. Biol. Chem. 270*, 10323−10327.

(14) Ahmed, M., Borsch, C. M., Taylor, S. S., Vazquez-Laslop, N., and Neyfakh, A. A. (1994) A Protein That Activates Expression of a Multidrug Efflux Transporter Substrates. *J. Biol. Chem. 269*, 28506−28513.

(15) Heldwein, E. E., and Brennan, R. G. (2001) Crystal structure of the transcription activator BmrR bound to DNA and a drug. *Nature 409*, 378−382.

(16) Kahmann, J. D., Sass, H.-J., Allan, M. G., Haruo, S., Thompson, C. J., and Grzesiek, S. (2003) Structural basis for antibiotic recognition by the TipA class of multidrug-resistance transcriptional regulators. *EMBO J. 22*, 1824−1834.

(17) Newberry, K. J., and Brennan, R. G. (2004) The Structural Mechanism for Transcription Activation by MerR Family Member Multidrug Transporter Activation, N Terminus. *J. Biol. Chem. 279*, 20356−20362.

(18) Newberry, K. J., Huffman, J. L., Miller, M. C., Vazquez-Laslop, N., Neyfakh, A. A., and Brennan, R. G. (2008) Structures of BmrR-Drug Complexes Reveal a Rigid Multidrug Binding Pocket and Transcription Activation through Tyrosine Expulsion. *J. Biol. Chem. 283*, 26795−26804.

(19) Baranova, N. N., Danchin, A., and Neyfakh, A. A. (1999) Mta, a global MerR-type regulator of the Bacillus subtilis multidrug-efflux transporters. *Mol. Microbiol. 31*, 1549−1559.

(20) Ansari, A. Z., Bradner, J. E., and O'Halloran, T. V. (1995) DNA-bend modulation in a repressor-to-activator switching mechanism. *Nature 374*, 371−375.

(21) Hidalgo, E., and Demple, B. (1997) Spacing of promoter elements regulates the basal expression of the *soxS* gene and converts SoxR from a transcriptional activator into a repressor. *EMBO, J. 16*, 1056−1065.

(22) Gaudu, P., and Weiss, B. (1996) SoxR, a [2Fe-2S] transcription factor, is active only in its oxidized form. *Proc. Natl. Acad. Sci. U. S. A. 93*, 10094−10098.

(23) Hidalgo, E., Ding, H., and Demple, B. (1997) Redox Signal Transduction: Mutations Shifting [2Fe-2S] Centers of the SoxR Sensor-Regulator to the Oxidized Form. *Cell 88*, 121−129.

(24) Ding, H., Hidalgo, E., and Demple, B. (1996) The Redox State of the [2Fe-2S] Clusters in SoxR Protein Regulates its Activity as a Transcription Factor. *J. Biol. Chem. 271*, 33173−33175.

(25) Hidalgo, E., Ding, H., and Demple, B. (1997) Redox signal transduction via iron-sulfur clusters in the SoxR transcription activator. *Trends Biochem. Sci. 22*, 207−210.

(26) Watanabe, S., Kita, A., Kobayashi, K., and Miki, K. (2008) Crystal structure of the [2Fe-2S] oxidative-stress sensor SoxR bound to DNA. *Proc. Natl. Acad. Sci. U. S. A. 105*, 4121−4126.
(27) Harada, I., and Takeuchi, H. (1986) *Raman and ultraviolet resonance Raman spectra of proteins and related compounds in Spectroscopy and Biological Systems* (Clark, R. J. H., and Hester, R. E., Eds.) pp 113−175, John Wiley, New York.
(28) El-Mashtoly, S. F., Takahashi, H., Shimizu, T., and Kitagawa, T. (2007) Ultraviolet Resonance Raman Evidence for Utilization of the Heme 6-Propionate Hydrogen-Bond Network in Signal Transmission from Heme to Protein in *Ec* DOS Protein. *J. Am. Chem. Soc. 129*, 3556−3563.
(29) Sato, A., Gao, Y., Kitagawa, T., and Mizutani, Y. (2007) Primary protein response after ligand photodissociation in carbonmonoxy myoglobin. *Proc. Natl. Acad. Sci. U. S. A. 104*, 9627−9632.
(30) Mizuno, M., Shibata, M., Yamada, J., Kandori, H., and Mizutani, Y. (2009) Picosecond Time-Resolved Ultraviolet Resonance Raman Spectroscopy of Bacteriorhodopsin: Primary Protein Response to Photoisomerization of Retinal. *J. Phys. Chem. B 113*, 12121−12128.
(31) Watanabe, S., Kita, A., Kobayashi, K., Takahashi, Y., and Miki, K. (2006) Crystallization and preliminary X-ray crystallographic studies of the oxidative-stress sensor SoxR and its complex with DNA. *Acta Crystallogr., Sect. F: Struct. Biol. Cryst. Commun. 62*, 1275−1277.
(32) Schlamadinger, D. E., Gable, J. E., and Kim, J. E. (2009) Hydrogen Bonding and Solvent Polarity Markers in the UV Resonance Spectrum of Tryptophan: Application to membrane Proteins. *J. Phys. Chem. B 113*, 14769−14778.
(33) Hashimoto, S., Obata, K., Takeuchi, H., Needleman, R., and Lanyi, J. K. (1997) Ultrviolet Resonance Raman Spectra of Trp-182 and Trp-189 in Bacteriorhodopsin: Novel Information on the Structure of Trp-182 and Its Steric Interaction with Retinal. *Biochemistry 36*, 11583−11590.
(34) Takeuchi, H. (2003) Raman structural markers of tryptophan and histidine side chains in proteins. *Biopolymers 72*, 305−317.
(35) Harada, I., Miura, T., and Takeuchi, H. (1986) Origin of the doublet at 1360 and 1340 cm^{-1} in the Raman spectra of tryptophan and related compounds. *Spectrochim. Acta, Part A 42*, 307−312.
(36) Miura, T., Takeuchi, H., and Harada, I. (1989) Tryptophan Raman Bands Sensitive to Hydrogen Bonding and Side-Chain Conformation. *J. Raman Spectrosc. 20*, 667−671.
(37) Miura, T., Takeuchi, H., and Harada, I. (1988) Characterization of Individual Tryptophan Side Chains in Proteins Using Raman Spectroscopy and Hydrogen-Deuterium Exchange Kinetics. *Biochemistry 27*, 88−94.
(38) Juszczak, L. J., and Desamero, R. Z. B. (2009) Extension of the Tryptophan $\chi^{2,1}$ Dihedral Angle-W3 Band Frequency Relationship to a Full Rotation: Correlations and Caveats. *Biochemistry 48*, 2777−2787.
(39) Haruta, N., and Kitagawa, T. (2001) Protein Conformation Change of Myogobin upon Ligand Binding Probed by Ultraviolet Resonance Raman Spectroscopy. *Biochemistry 41*, 6595−6604.
(40) Fodor, S. P., Rava, R. P., Hays, T. R., and Spiro, T. G. (1985) Ultraviolet Resonance Raman Spectroscopy of DNA with 200−266-nm Laser Excitation. *J. Am. Chem. Soc. 107*, 1520−1529.
(41) Perno, J. P., Grygon, C. A., and Spiro, T. G. (1989) Ultraviolet Raman Excitation Profiles for the Nucleic Acid Duplexes Poly(rA)-Poly(rU) and Poly(dG-dC). *J. Phys. Chem. 93*, 5672−5678.
(42) Mukerji, I., and Williams, A. P. (2002) UV Resonance and Circular Dichroism Studies of a DNA Duplex Containing an A_3T_3 Tract: Evidence for a Premelting Transition and Three-Centered H-Bonds. *Biochemistry 41*, 69−77.
(43) Chen, J., Bender, S. L., Keough, J. M., and Barry, B. A. (2009) Tryptophan as a Probe of Photosystem I Electron Transfer Reactions: A UV Resonance Raman Study. *J. Phys. Chem. B 113*, 11367−11370.
(44) Matsuno, M., and Takeuchi, H. (1998) Effect of Hydrogen Bonding and Hydrophobic Interactions on the Ultraviolet Resonance Raman intensities of Indole Ring Vibrations. *Bull. Chem. Soc. Jpn. 71*, 851−857.
(45) Fujisawa, T., Terajima, M., and Kimura, Y. (2006) Excitation wavelength dependence of the Raman-Stokes shift of *N, N*-dimethyl-*p*-nitroaniline. *J. Chem. Phys. 124*, 184503−184509.
(46) Schoute, L. C. T., Helburn, R., and Kelley, A. M. (2007) Solvent Effects on the Resonance Raman and Hyperpolarizability of *N, N*-dimethyl-*p*-nitroaniline. *J. Phys. Chem. A 111*, 1251−1258.
(47) Xue, Y., Davis, A. V., Balakrishnan, G., Stasser, J. P., Staehlin, B. M., Focia, P., Spiro, T. G., Penner-Hahn, J. E., and O'Halloran, T. V. (2008) Cu(I) recognition via cation-π and methionine interactions in CusF. *Nat. Chem. Biol. 4*, 107−109.
(48) Wen, Z. Q., and Thomas, G. J. Jr. (2000) Ultraviolet-Resonance Raman Spectroscopy of Filamentous Virus Pf3: interactions of Trp 38 Specific to the Assembled Virion Subunit. *Biochemistry 39*, 146−152.
(49) Okada, A., Miua, T., and Takeuchi, H. (2001) Protonation of Histidine-Tryptophan Interaction in the Activation of the M2 Ion Channel from Influenza A Virus. *Biochemistry 40*, 6053−6060.
(50) Kumaraswami, M., Newberry, K. J., and Brennan, R. G. (2010) Conformational Plasticity of the Coiled-Coil Domain of BmrR is Required for *bmr* Operator Binding: The Structure of Unliganded BmrR. *J. Mol. Biol. 398*, 264−275.
(51) Song, L., Teng, Q., Phillips, R. S., Brewer, J. M., and Summers, A. O. (2007) ^{19}F-NMR Reveals Metal and Operator-induced Allostery in MerR. *J. Mol. Biol. 371*, 79−92.
(52) Rodgers, K. R., Su, C., Subramaniam, S., and Spiro, T. G. (1992) Hemoglobin R→T Structural Dynamics from Simultaneous Monitoring of Tyrosine and Tryptophan Time-Resolved UV Resonance Raman Signals. *J. Am. Chem. Soc. 114*, 3697−3709.
(53) Takeuchi, H., Watanabe, M., Satoh, Y., and Harada, I. (1989) Effects of hydrogen bonding on the tyrosine Raman bands in the 1300−1150 cm^{-1} region. *J. Raman Spectrosc. 20*, 233−237.
(54) Gorodetsky, A. A., Dietrich, L. E. P., Lee, P. E., Demple, B., Newman, D. K., and Barton, J. K. (2008) DNA binding shifts the redox potential of transcription factor SoxR. *Proc. Natl. Acad. Sci. U. S. A. 105*, 3684−3689.
(55) Morales, R., Charon, M. H., Hudry-Clergeon, G., Petillot, Y., Norager, S., Medina, M., and Frey, M. (1999) Refined X-ray structures of the oxidized, at 1.3 Å, and reduced, at 1.17 Å, [2Fe-2S] ferredoxin from the *cynobacteroum Anabaena* PCC7119 show redox-linked conformational change. *Biochemistry 38*, 15764−15773.
(56) Sevrikoukova, I. F. (2005) Redox-dependent structural reorganization in putidaredoxin, a vertebrate-type [2Fe-2S] ferredoxin from *Pseudomonas putida*. *J. Mol. Biol. 347*, 607−621.
(57) Noodleman, L., Peng, C. Y., Case, D. A., and Mouesca, J.-M. (1995) Orbital interactions, electron delocalization and spin coupling in iron-sulfur clusters. *Coord. Chem. Rev. 144*, 199−244.
(58) Newberry, K. J., Huffman, J. L., Miller, M. C., Vazquez-Laslop, N., Neyfakh, A. A., and Brennan, R. G. (2008) Structures of BmrR-Drug Complexes Reveal a Rigid Multidrug Binding Pocket and Transcription Activation through Tyrosine Expulsion. *J. Biol. Chem. 283*, 26795−26804.